J Therm Anal Calorim (2010) 100:917–923
DOI 10.1007/s10973-009-0381-0

Thermal behavior of titania grafted with phosphonic acids under non-isothermal conditions

Gheorghe Ilia · Madalina Drehe · Titus Vlase · Gabriela Vlase · Lavinia Macarie · Nicolae Doca

Received: 28 April 2009 / Accepted: 22 July 2009 / Published online: 28 August 2009

Abstract Metal or metal oxide nanoparticles possess unique features compared to equivalent larger-scale materials. In this paper we present the synthesis of grafted titania with phosphonic acids, their characterization and an extended non-isothermal kinetic study. The obtained results show that there in no significant difference between acids and esters in grafting reaction. The phosphorus content wary between 0.9 and 1.80% and is comparable with literature data. IR and AFM studies confirmed the formation of grafted titania. Extended non-isothermal kinetic study using different methods confirmed the complexity of thermooxidative degradation processes in non-isothermal conditions.

Keywords Titania · Grafted · Phosphonic · Non-isothermal kinetic

Introduction

Metal or metal oxide nanoparticles possess unique features compared to equivalent larger-scale materials. For applications, it is often necessary to stabilize or functionalize such nanoparticles. Thus, modification of the surface of nanoparticles is an important chemical challenge [1].

The synthesis of organic–inorganic hybrid materials aims to combine the physical and chemical properties of inorganic and organic components. Moreover for many applications (such as catalysis, chromatography, ion extraction, etc.), inorganic and organic components have to be strongly linked together, via covalent or ionic-covalent bonds [2–4].

Grafted metal oxide surfaces with phosphonic acids $RPO(OH)_2$ has numerous applications: self-assembled monolayers [5], ceramic membrane [6, 7], binding of photosensitise materials to TiO_2 in solar energy conversion systems [8].

The grafting was achieved by treating a suspension of TiO_2 particles at room temperature with an aqueous solution of phosphonic or phosphinic acids [9, 10]. In the case of TiO_2, the pH was adjusted to 3.5, in order to be far from pH 5.9, the value of zero-charge state for TiO_2, so that electrostatic repulsive forces due to charged surface sites acted between the particles, giving unaggregated suspensions [11].

In this paper we present the synthesis of grafted titania with phosphonic acids (different from those mentioned before in literature), their characterization and an extended non-isothermal kinetic study, which to our knowledge has not been reported. Alike as many heterogeneous materials, the grafted titania surface is thermosensitive, the thermal behavior is rather a compulsory task.

Experimental

Reagents

Phosphorus acid, diethyl cyanomethyl phosphonate, diethylbenzyl phosphonate, methanol and toluene were reagent grade (Aldrich) and used as received. Styryl phosphonic acid was synthesised in our laboratory. Titania

G. Ilia (✉) · L. Macarie
Institute of Chemistry Timisoara, 24 Mihai Viteazul Str., 300224 Timisoara, Romania
e-mail: ilia@acad-icht.tm.edu.ro; gheilia@yahoo.com

G. Ilia · M. Drehe · T. Vlase · G. Vlase · N. Doca
Faculty of Chemistry, Biology and Geography, West University, 116 Pestalozzi Str., 300115 Timisoara, Romania

TR-95 was commercially one and was supplied by Azur SA Timisoara and has the following characteristics: TiO_2—92%; dimension of particles—0.23 μm; density—1.2 g cm^{-3}; mass loss at 105 °C—0.6%.

Preparation of grafted titania using phosphorus and styryl phosphonic acids

The sample were prepared using 1.6×10^{-3} mol of coupling molecules per gram of TiO_2.

To the required quantitiy of inorganic oxide suspended in 100 mL water the calculated quantity of phosphorus acid disoved in an apropriate solvent (water or water–methanol) is added and the mixture is kept under stirring. The pH was adjusted at 3–3.5. After modification, the anchored particles were filtered off, washed successively with methanol, acetone, and diethyl ether (to remove unreacted or physisorbed coupling molecules), and dried under vacuum (120 °C, 5 h, 10^{-2} mbar).

Preparation of grafted titania using phosphonic esters

The sample were prepared using 1.6×10^{-3} mol of coupling molecules per gram of TiO_2.

To the required quantity of inorganic oxide suspended in toluene is added and the mixture is kept under stirring. After modification, the anchored particles were filtered off, washed successively with methanol, acetone, and diethyl ether (to remove unreacted or physisorbed coupling molecules), and dried under vacuum (120 °C, 5 h, 10^{-2} mbar).

Analysis

The obtained hybrids were characterized by Fourier transform infrared spectroscopy with a Jasco 430 spectrometer (spectral range 4,000–400 cm^{-1}, 256 scans, and resolution 2 cm^{-1}) using KBr pellets and atomic force microscopy (AFM) with Nanosurf1 Easy-Scan 2 Advanced Research microscope.

A Perkin-Elmer DIAMOND device was used for thermal analysis, with Al crucible, dynamic air atmosphere (100 mL min^{-1}) and heating rates of $\beta = 5$, 10, 12 and 15 °C min^{-1}.

Determination of phosphorus content

A sample of the final product precisely weighted was burnt out in an oxygen atmosphere and the P_2O_5 formed was absorbed in water. The solution obtained was titrated with an aqueous solution of cerium (III) 0.005 M in the presence of Eryochrome Black T as indicator.

Results and discussion

Depending on the chemical stability of the oxide and the reaction conditions (temperature, concentration, pH, and nature of the solvent) a dissolution–precipitation process may compete with surface modification, leading to the formation of a metal phosphonate.

The reaction conditions and the obtained results for phosphorus acid, styryl phosphonic acid, diethyl-cyanomethyl phosphonate and diethylbenzyl phosphonate grafted on titania are presented in Table 1.

Elemental analysis showed the presence of phosphorus in all the samples, indicating that all of the coupling molecules did react with the surface of the inorganic oxide particles and giving accurate indication of the amount of organophosphorus units present on the surface of the particles.

Regardless of the type of phosphonate coupling molecule used, the IR spectra of the modified particles present close typical features, with a strong band near 1,140 cm^{-1}, characteristic of P–C groups (except phosphorus acid in which spectrum appears a band at 2,290–2,320 cm^{-1} corresponding to P–H bond) and broad P–O stretching bands between 890 and 1,180 cm^{-1}. A weak band at 3,060 cm^{-1}, characteristic of the aromatic C–H, is also present. For styryl phosphonic acid appears a band near 1,600 cm^{-1} and for cyanomethyl phosphonate a band near 2,250 cm^{-1}. The O–H stretching bands at 3,700 and 3,500 cm^{-1}, associated with Ti–OH groups and adsorbed water, appear as negative bands in the subtracted spectra of the modified particles, which is consistent with condensations involving Ti–OH groups and with a decrease in the surface hydrophilicity. The significant decrease of the vibrations typical of P–OH, and P–OEt groups suggests that the condensation of these groups with Ti–OH surface groups is practically complete.

Table 1 Reaction conditions and the obtained results for grafted titania

Product	Phosphorus derivative	*g* phosphorus derivative/g TiO_2	Solvent/mL	Temp./°C	Time/h	P/%	% grafted phosphorus derivative
TR-H_3PO_3	Phosphorus acid 30%	10/35	Water, 100	20–25	24	1.70	4.50
TR-styryl	Styryl phosphonic acid	5/5	Methanol/water: 50/50	20–25	24	0.92	5.54
TR-cyano	Diethyl-cyanomethyl phosphonate	5/5	Toluene, 50	55–60	20	1.74	9.95 (0.78%N)
TR-benzyl	Diethylbenzyl phosphonate	5/5	Toluene, 50	55–60	20	1.16	8.50

According to the literature data, the anchoring implies the formation of Ti–O–P bridge from the P = O or P–O– bonds [9]. The most probable bonding mode is bidentate one [12].

For all products AFM images were recorded (Figs. 1, 2, 3, 4, 5). The recorded AFM images show an increase in dimension of grafted inorganic supports comparatively with non grafted commercial titania.

The TG, DTG and DTA curves at heating rate 10 °C min^{-1} are presented in Figs. 6, 7, 8, 9 and the main thermal characteristics of the synthesized compounds are systematized in Table 2. The mass loss observed until 100 °C is probably due to a supplementary esterification between Ti–OH and P–OH groups, and this step was not taken into account for the kinetic study.

The most thermostable material is TR-styryl, and this probably due to the extended conjugation from the aromatic ring to the phosphorus atom. The absence of such conjugation leads to a less thermostable TR-benzyl. Another important observation is the high exothermicity by the thermooxidation of the organic anchored materials.

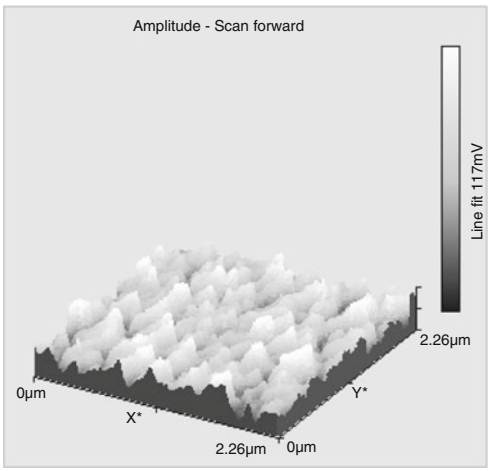

Fig. 1 2D representation of TR92. 3D map

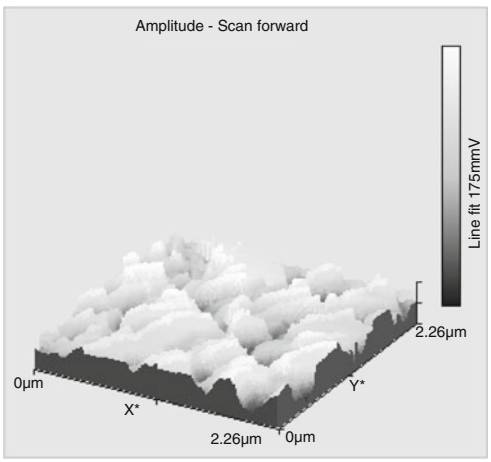

Fig. 2 2D representation of TR-H_3PO_3. 3D map

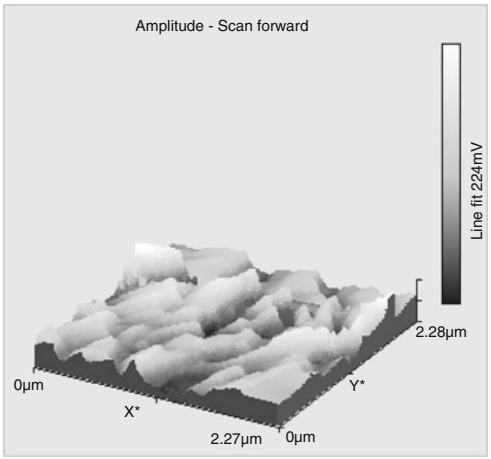

Fig. 3 2D representation of TR-styryl. 3D map

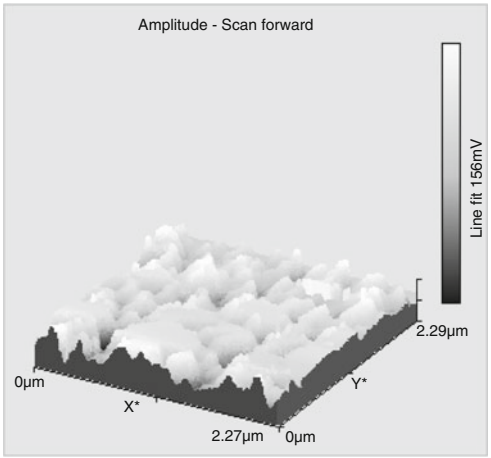

Fig. 4 2D representation of TR-cyano. 3D map

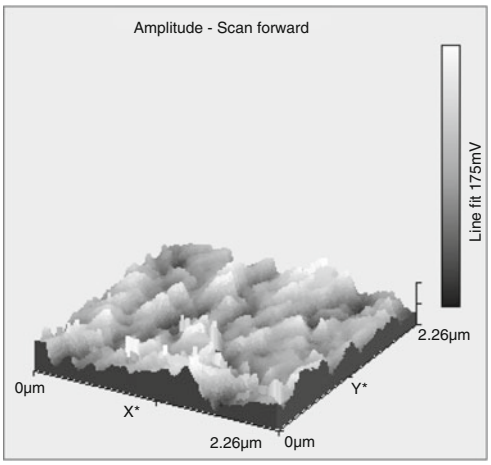

Fig. 5 2D representation of TR-benzyl. 3D map

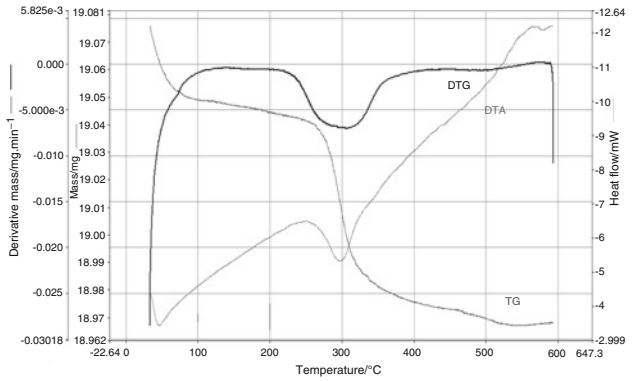

Fig. 6 TG, DTG and DTA curves for TR-H_3PO_3

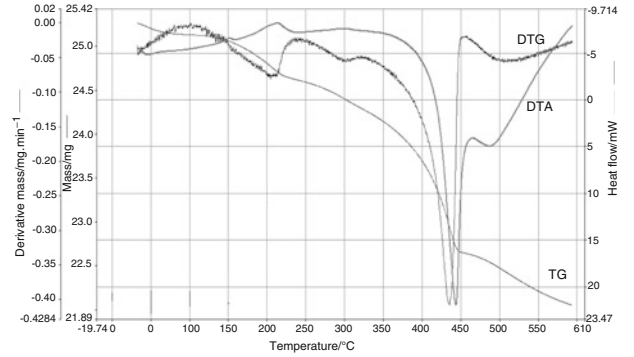

Fig. 7 TG, DTG and DTA curves for TR-styryl

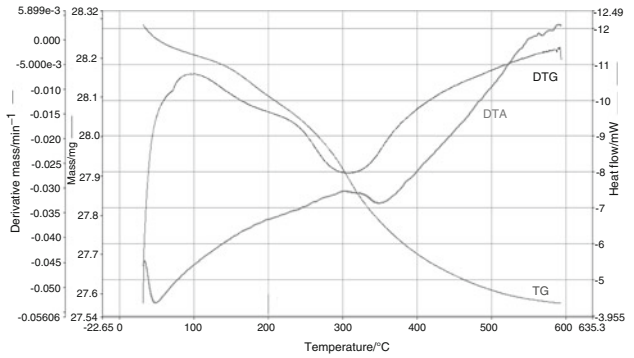

Fig. 8 TG, DTG and DTA curves for TR-cyano

This is evidenced by the remarkable differences between max DTG and max DTA.

Unfortunately these information are rather insufficient, so that a kinetic analysis was suggested which is expected to produce an adequate description of processes in terms of the Arrhenius parameters and the reaction model:

$$\frac{d\alpha}{dt} = k(T) \cdot f(\alpha) \quad (1)$$

where t, time; T, temperature; α, conversion degree; $f(\alpha)$, reaction model.

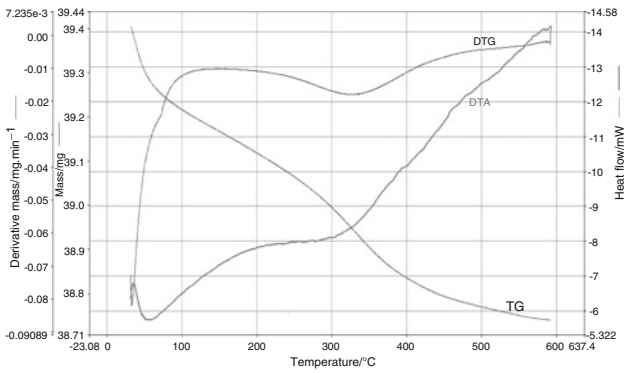

Fig. 9 TG, DTG and DTA curves for TR-benzyl

Table 2 The thermal characteristics of the prepared samples by heating rate of 10 °C min^{-1}

Sample	$T_{initial}$/°C	T_{final}/°C	Max DTG/°C	Max DTA/°C	Mass loss/%
TR-H_3PO_3	244	383	301	300	0.35
TR-styryl	266	459	434	444	7.60
TR-cyano	221	557	303	351	1.80
TR-benzyl	208	486	328	302	0.85

Kinetic analysis

We expected that the thermooxidation is a multi-step process, so isoconversional method will be used by processing the experimental data. At the beginning we decided to use model free methods that allow the evolution of Arrhenius parameters without choosing the reaction model.

The Flynn–Wall [13] and Ozawa [14] (FWO) method

The method requires the temperature measurements at certain conversions α for experiments at different heating rates. By non-isothermal conditions $d\alpha/dt$ in Eq. 1 is replaced with $\ln\beta d\alpha/dt$, so that the integrated form of Eq. 1 becomes:

$$\ln \beta = \ln \frac{AE}{Rg(\alpha)} - 5.331 - 1.052 \cdot \frac{E}{RT} \quad (2)$$

where $g(\alpha) = \int_{\alpha_0}^{\alpha} \frac{d\alpha}{f(\alpha)}$, α is the conversion, β the heating rate, and A, E the Arrhenius kinetic parameters.

From the slope of the straight line of $\ln \beta$ versus $1/T$ the activation energy E for different conversion degrees will be obtained.

In Fig. 10 is presented the variation of activation energy function of conversion for all grafted phosphonates and show a significant variation of E versus α, this being an indication of complex multi-step processes.

According to a suggestion of Vyazovkin and Lesnikovich [15] for TR-H_3PO_3 a successive sequence of reaction

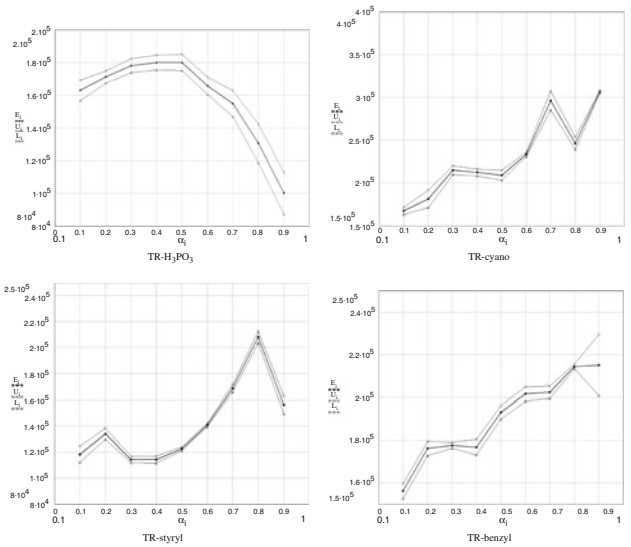

Fig. 10 Variation of activation energy versus conversion degree with confidence interval obtained by FWO method

take place; for TR-styryl and TR-benzyl there are parallel reactions with mechanism change at $\alpha = 0.3$, and $\alpha = 0.4$, respectively. The case of TR-cyano is to complicate for this rather qualitative estimation.

Friedman's method [16]

The method is an isoconversional-differential one and is based on the equation:

$$\ln\left(\beta \cdot \frac{\mathrm{d}\alpha}{\mathrm{d}T}\right)_{\alpha} = \ln[A \cdot f(\alpha)] - \frac{E}{RT} \tag{3}$$

Because $f(\alpha)$ is not explicit, Friedman's method is a model free method. By plotting the left member of Eq. 3 (DTG values) versus $1/T$, the activation energy at certain conversion is obtained (Fig. 11).

Friedman method confirms the existence of successive reactions for TR-H_3PO_3, a sequence of reactions for TR-styryl. The high variation of activation of energy function of conversion for TR-cyano sustains the hypothesis of a multistage process. In the case of TR-benzyl the variation of activation of energy function of conversion is confirmed.

NPK method [17–19]

Based on our previous results [20–23], the kinetic analysis was continued with the Non Parametric Kinetics (NPK) method. We selected this method due to its ability in separation two or more elementary steps of a complex process and also because this method is not restricted to the mathematical equation of the kinetic model.

By this method, the experimental points obtained at different heating rates β, are represented in a 3D space with

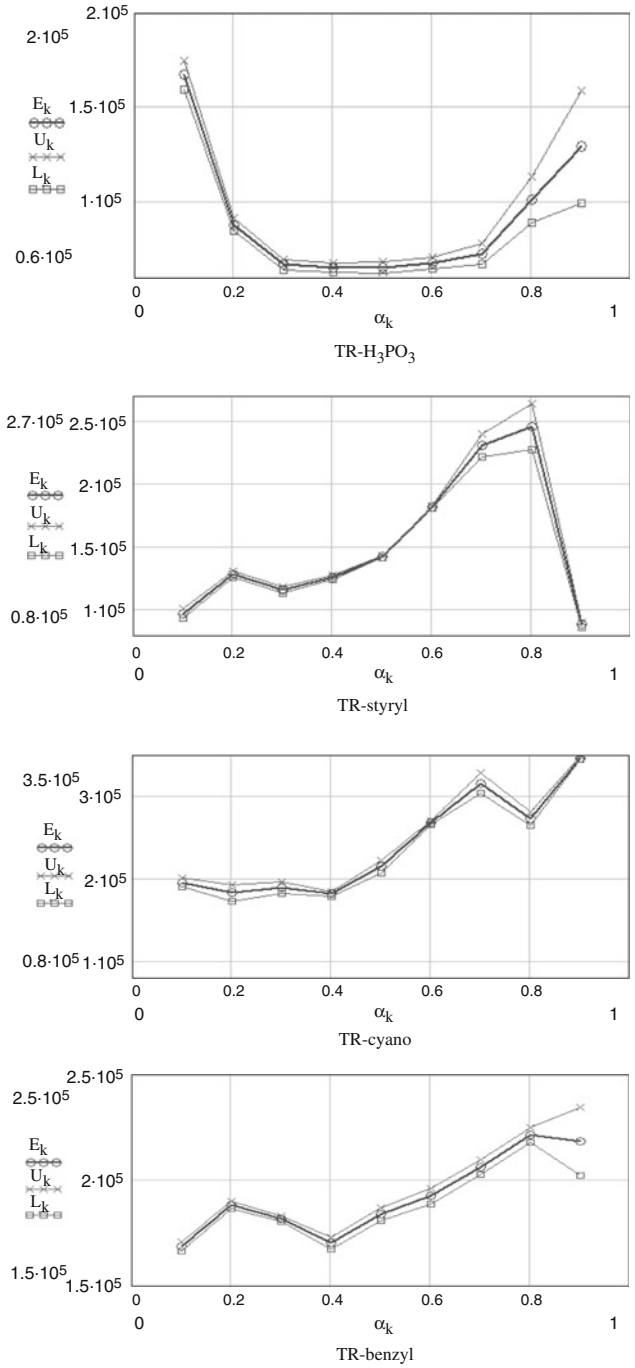

Fig. 11 Variation of activation energy versus conversion degree with confidence interval obtained by FR method

the coordinates of (T_j, α_i, r_{ij}), in accordance with the fundamental hypothesis that the reaction rate can be expressed as a product of two separable functions

$$r_{ij} = k(T_j) \cdot g(\alpha_i) \tag{1}$$

These points are interpolated by a proper algorithm and a continuous surface of the reaction rate is obtained.

Table 3 Kinetic parameters obtained by NPK method

Product	λ	E/kJ mol^{-1}	A/min^{-1}	m	n	$\bar{E} = \sum(\lambda \cdot E)/$ kJ mol^{-1}
TR-H_3PO_3	97.7	29.1	124.5	1/2	–	34.3
	2.2	266.6	3.19×10^{22}	–	2	
TR-styryl	61.2	141.7	3.7×10^{15}	–	1	120.98
	38.5	89.0	4.6×10^{9}	1	–	
TR-cyano	80.7	112.7	5.5×10^{8}	–	2/3	108.8
	19.2	92.9	1.5×10^{7}	2	–	
TR-benzyl	77.0	126.5	6.8×10^{10}	2	2/3	116.9
	15.8	59.1	4.2×10^{4}	1	1	

This surface can be suitable discretizated into an *ixj* square matrix

$$M = \{r_{i,j}\} \quad (2)$$

or, in accordance with Eq. 1

$$M = \{g(\alpha_i) \cdot k(T_j)\} \quad (3)$$

The NPK method uses the Singular Value Decomposition (SVD) algorithm [24] to decompose the matrix M:

$$M = U\,(\text{diag } S)V^{\text{T}} \quad (4)$$

In this way, the influence of the conversion and temperature respectively, are separated since:

- a vector $\mathbf{u}_1$ given by the first column of the matrix U is analyzed versus α to determine the conversion function $g(\alpha)$; we suggest the Sestak–Berggren equation [25]:

$$g(\alpha) = \alpha^m(1-\alpha)^n \quad (5)$$

- a vector $\mathbf{v}_1$ given by the first column of the matrix V is searched for the temperature dependence $f(T)$; a classical Arrhenius equation was suggested.

By applying the SVD algorithm, also a separation of two or more simultaneous steps of a complex process is possible. Indeed, if the observed reaction rate al α_i and T_j is a result of two simultaneous reactions with the rates r_1 and r_2, it means that

$$r_{ij} = r_1(ij) + r_2(ij) = g_1(\alpha_i) \cdot k_1(T_j) + g_2(\alpha_i) \cdot k_2(T_j) \quad (6)$$

and the corresponding matrix M became

$$M = U_1(\text{diag } S_1)V_1^{\text{T}} + U_2(\text{diag } S_2)\,V_2^{\text{T}} \quad (7)$$

In the same manner, two independent vectors $\mathbf{u}_1$ and $\mathbf{u}_2$ for the conversion function, respectively two independent vectors $\mathbf{v}_1$ and $\mathbf{v}_2$ for the temperature dependence should be obtained.

The contribution of each step to the total process is quantitatively expressed by the explained variance λ_i, so that $\Sigma\lambda_i = 100\%$. The data were summarized in Table 3. Only the processes with $\lambda > 10\%$ are considered as significant.

It is obvious that, except TR-H_3PO_3, the other three materials presents two parallel processes, the first one having the higher activation energy (in the range of 110–140 kJ mol^{-1}).

If we consider a mean value $\bar{E} = \Sigma(\lambda_i E_i)$ of the both steps, the values of activation energy are very near (105–120 kJ mol^{-1}) and significantly different from that for TR-H_3PO_3. This means that the influence of temperature on the thermooxidative degradation of the organic-containing materials is rather the same and very different from the inorganic TR-H_3PO_3.

Regarding the conversion function, the four materials had different behavior: for TR-H_3PO_3 only a physical phenomenon is responsible for thermodegradation ($m \neq 0$, $n = 0$), this being the reason for low value of E; for organic-containing materials the preponderant degradation step is a chemical one ($n = 0.66$–1.0) and a secondary step, especially of physical relevance ($m = 1$), accompany the chemical thermooxidation.

The NPK method allowed a better description of the complex kinetic behavior and took into account the observed differences from the TG/DTG curve, especially that due to the kinetic model. The narrow range of E values, by organic compounds, indicates a similar mechanism of thermooxidative degradation, probably beginning with the breaking of the P–C bonds.

Conclusions

In this paper phosphonic acids and esters were used for obtaining grafted titania. The obtained results show that there in no significant difference between acids and esters in grafting reaction. The phosphorus content wary between 0.9 and 1.80% and is comparable with literature data. The use of organic solvents in the case of esters is advantageous

because reduces fotodegradation of titania. IR and AFM studies confirmed the formation of grafted titania. Extended non-isothermal kinetic study using different methods confirmed the complexity of thermooxidative degradation processes in non-isothermal conditions. The reaction sequences were interpreted and kinetic parameters were identified. Using modified NPK method permitted the separation of influence of temperature and conversion degree, and most important, allowed the identification and separation of two or more steps of complex processes without any "a priori" hypotheses.

The performed kinetic analysis was useful for a complete characterization of the thermooxidative behavior of the studied materials. Indeed, at first, a clear difference of the activation energy between inorganic, respectively organic anchoring compounds was evidenced. Then, the differences in the kinetic model accounts for the different thermooxidation rate of the organo-phosphonic compounds.

References

1. Neouze MA, Schubert U. Surface modification and functionalization of metal and metal oxide nanoparticles by organic ligands. Monatsh Chem. 2008;139:183–95.
2. Mingalyov PG, Lisichkin GV. Chemical modification of oxide surfaces with organophosphorus(V) acids and their esters. Russ Chem Rev. 2006;75:541–57.
3. Mutin PH, Guerrero G, Vioux A. Hybrid materials from organophosphorus coupling molecules. J Mater Chem. 2005;15:3761–8.
4. Vioux A, Mutin PH, Le Bideau J, Leclercq D. Organophosphorus-based organic/inorganic hybrids. Mat Res Soc Symp Proc. 2000;628:CC1.4.1–4.12.
5. Gao W, Dickinson L, Grozinger C, Morin FG, Reven L. Self-assembled monolayers of alkylphosphonic acids on metal oxides. Langmuir. 1996;126:429–6435.
6. Randon J, Blanc P, Paterson R. Modification of ceramic membrane surfaces using phosphoric acid and alkyl phosphonic acids and its effects on ultrafiltration of BSA protein. J Membr Sci. 1995;98:119–29.
7. Caro J, Noack M, Kolsch P. Chemically modified ceramic membranes. Microporous Mesoporous Mater. 1998;22:321–32.
8. Zakeeruddin SM, Nazeeruddin MK, Pechy P, Rotzinger FP, Humphrybaker R, Kalyanasundaram K, et al. Molecular engineering of photosensitizers for nanocrystalline solar cells: synthesis and characterization of Ru dyes based on phosphonated terpyridines. Inorg Chem. 1997;36:5937–46.
9. Guerrero G, Mutin PH, Vioux A. Anchoring of phosphonate and phosphinate coupling molecules on titania particles. Chem Mater. 2001;13:4367–73.
10. Guerrero G, Chaplais G, Mutin PH, Le Bideau J, Leclercq D, Vioux A. Grafting of alumina by diphenylphosphinate coupling agents. Mat Res Soc Symp Proc. 2000;628:CC6.6–CC6.6.1.
11. Tombácz E, Szekeres M, Kertész I, Turi L. pH-dependent aggregation state of highly dispersed alumina, titania and silica particles in aqueous medium. Prog Colloid Polym Sci. 1995;98:160–8.
12. Funar-Timofei S, Ilia G. Simulation of grafting reaction of benzyl phosphonic acid on titanium oxide by the semiempirical PM6 approach. J Opt Adv Mater. 2008;10:2649–52.
13. Flynn IH, Wall LA. A quick, direct method for the determination of activation energy from thermogravimetric data. J Polym Sci Part B. 1966;4:323–8.
14. Ozawa T. A new method of analyzing thermogravimetric data. Bull Chem Soc Jpn. 1965;38:1881–6.
15. Vyazovkin S, Lesnikovich AI. Practical application of isoconversional methods. Thermochim Acta. 1992;203:177–85.
16. Friedman HL. New methods for evaluating kinetic parameters from thermal analysis data. J Polym Sci. 1969;7:41–6.
17. Serra R, Nomen R, Sempere J. The non-parametric kinetics a new method for the kinetic study of thermoanalytical data. J Therm Anal Calorim. 1998;52:933–43.
18. Serra R, Sempere J, Nomen R. A new method for the kinetic study of thermoanalytical data: the non-parametric kinetics method. Thermochim Acta. 1998;316:37–45.
19. Sempere J, Nomen R, Serra R. Progress in non-parametric kinetics. J Therm Anal Calorim. 1999;56:843–9.
20. Ioitescu A, Vlase G, Vlase T, Doca N. Kinetics of decomposition of different acid calcium phosphates. J Therm Anal Calorim. 2007;88:121–5.
21. Vlase T, Vlase G, Birta N, Doca N. Comparative results of kinetic data obtained with different methods for complex decomposition steps. J Therm Anal Calorim. 2007;88:631–5.
22. Birta N, Doca N, Vlase G, Vlase T. Kinetic of sorbitol decomposition under non-isothermal conditions. J Therm Anal Calorim. 2008;92:635–8.
23. Vlase T, Vlase G, Doca N. Thermal behavior of some phenitoine pharmaceuticals. J Therm Anal Calorim. 2008;92:259–62.
24. Wall ME. A practical approach to microarray data analysis, vol. 9. Norwel: Kluwer. LANL LA-UR-02; 2003. p. 91–109.
25. Sestak J, Berggren G. Study of the kinetics of the mechanism of solid-state reactions at increasing temperatures. Thermochim Acta. 1971;3:1–12.